Eur Biophys J (2009) 38:625–635
DOI 10.1007/s00249-009-0420-6

ORIGINAL PAPER

Rapid folding of the prion protein captured by pressure-jump

David C. Jenkins · David S. Pearson · Andrew Harvey · Ian D. Sylvester · Michael A. Geeves · Teresa J. T. Pinheiro

Received: 10 November 2008 / Revised: 16 January 2009 / Accepted: 29 January 2009 / Published online: 3 March 2009

Abstract The conversion of the cellular form of the prion protein (PrP^C) to an altered disease state, generally denoted as scrapie isoform (PrP^{Sc}), appears to be a crucial molecular event in prion diseases. The details of this conformational transition are not fully understood, but it is perceived that they are associated with misfolding of PrP or its incapacity to maintain the native fold during its cell cycle. Here we present a tryptophan mutant of PrP (F198W), which has enhanced fluorescence sensitivity to unfolding/refolding transitions. Equilibrium folding was studied by circular dichroism and fluorescence. Pressure-jump experiments were successfully applied to reveal rapid submillisecond folding events of PrP at temperatures not accessed before.

Keywords Prion folding · Folding intermediate · Pressure-jump · Tryptophan mutant · Folding kinetics · Prion conversion

Abbreviations

CD	Circular dichroism
GdnHCl	Guanidine hydrochloride
NMR	Nuclear magnetic resonance
PrP	Prion protein
SHaPrP	Syrian hamster prion protein

D. C. Jenkins and D. S. Pearson contributed equally.

D. C. Jenkins · A. Harvey · I. D. Sylvester · T. J. T. Pinheiro (✉)
Department of Biological Sciences, University of Warwick, Gibbet Hill Road, Coventry CV4 7AL, UK
e-mail: t.pinheiro@warwick.ac.uk

D. S. Pearson · M. A. Geeves
Department of Biosciences, University of Kent, Canterbury, Kent CT2 7NJ, UK

Introduction

Transmissible spongiform encephalopathies, which include Creutzfeldt-Jakob disease (CJD) in humans, bovine spongiform encephalopathy in cattle, and scrapie in sheep, are associated with the conversion of the normal cellular form of the prion protein (PrP^C) to an altered pathological form, generally referred to as the scrapie isoform (PrP^{Sc}). These diseases are also known as prion diseases and can occur as sporadic, inherited or be acquired through transmission. Sporadic CJD accounts for 85% of all cases of disease; around 10–15% are associated with the familial cases and less than 5% are transmitted (Collinge 2005).

According to the prion hypothesis (Bolton et al. 1982; Prusiner 1998) the pathological isoform can self-replicate by associating with the cellular form and converting PrP^C to PrP^{Sc} through a template-assisted mechanism (Prusiner et al. 1998). The details of prion conversion are not fully understood, but it is generally accepted that this transformation involves a refolding of PrP from its cellular normal state to the altered disease-associated form. Thus, studies of the unfolding and refolding mechanisms of PrP should provide invaluable insight into the process of prion conversion.

PrP^C and PrP^{Sc} are the product of the same gene (Chesebro et al. 1985; Oesch et al. 1985) with identical posttranslational modifications (Stahl et al. 1993), but their secondary and tertiary structures contrast greatly. Whereas PrP^C contains a long unstructured N-terminal region and a globular C-terminal domain, composed of three α-helices and two short β-strands (Donne et al. 1997; James et al.

1997; Liu et al. 1999; Riek et al. 1996), PrP^{Sc} has a much higher proportion of β-sheet structure (Pan et al. 1993). Physicochemical studies have shown that PrP^{C} is monomeric, soluble in aqueous buffers and fully degraded by proteases, whereas PrP^{Sc} is a polymeric aggregated state, insoluble in water and detergents, and resistant to proteinase K digestion (McKinley et al. 1983; Meyer et al. 1986; Oesch et al. 1985).

It is apparent that the underlying fundamental mechanism of prion conversion in transmissible spongiform encephalopathies (TSEs), either under template-assisted through contact with PrP^{Sc} in transmitted cases or during spontaneous conversion in sporadic and familial cases, involves a major refolding of the protein from its α-helical PrP^{C} state to the β-sheet-rich conformation associated with PrP^{Sc}. Therefore, the study of prion folding has attracted efforts from several groups using a wide range of biophysical approaches. Several wild-type recombinant constructs of PrP and their mutants have been subjected to equilibrium folding studies by fluorescence (Cordeiro et al. 2005b; Jenkins et al. 2008; Wildegger et al. 1999), circular dichroism (CD; Apetri et al. 2004; Hornemann and Glockshuber 1998; Hosszu et al. 2005; Jackson et al. 1999; James et al. 1997; Liemann and Glockshuber 1999; Swietnicki et al. 1997, 1998; Wildegger et al. 1999; Zhang et al. 1997), infrared (Cordeiro et al. 2005a; Font et al. 2006), and nuclear magnetic resonance spectroscopy (Hosszu et al. 2005; Zhang et al. 1997). In these equilibrium studies unfolding and refolding transitions are induced by external factors such as chemical denaturants (Cordeiro et al. 2005b; Hornemann and Glockshuber 1998; Hosszu et al. 2005; Jackson et al. 1999; Jenkins et al. 2008; Liemann and Glockshuber 1999; Swietnicki et al. 1997, 1998; Zhang et al. 1997), pH (Hornemann and Glockshuber 1998), temperature (Cordeiro et al. 2005a,b; Jackson et al. 1999; Swietnicki et al. 1998; Zhang et al. 1997) and pressure (Alvarez-Martinez et al. 2003; Cordeiro et al. 2005a, b; Kuwata et al. 2002). Although these studies have produced detailed thermodynamic parameters for the folding at equilibrium, very few studies exist on the folding kinetics of PrPs.

Using stopped-flow fluorescence, two separate groups have reported that the C-terminal domain of PrP folds very rapidly (Apetri and Surewicz 2002; Wildegger et al. 1999). Folding kinetics were only captured at low temperature (4–5°C) and were not observable at higher temperatures because the unfolding and refolding transitions for PrP are too fast to be captured within the detection time of stopped-flow instrumentation (above 1 ms). A recent study using a continuous-flow instrument (Apetri et al. 2006) has detected an early kinetic intermediate in the folding pathway of PrP at low temperature (Apetri et al. 2004; Apetri and Surewicz 2002). To date, no kinetic studies of the folding of PrP have been conducted at temperatures approaching that of physiological conditions.

In the current study, we describe the folding and stability of a tryptophan mutant (F198W) of truncated PrP (residues 90–231 of the Syrian hamster protein), containing the folded C-terminal domain. Through equilibrium measurements by fluorescence spectroscopy and CD we show that the mutant protein has a similar fold and thermodynamic stability as the wild-type protein. Fast submillisecond folding kinetic events in the folding of PrP at 20°C were captured through equilibrium perturbation pressure-jump measurements.

Materials and methods

Mutagenesis and protein purification

The plasmid (pIngPrP) encoding the Syrian hamster PrP was originally prepared by Mehlhorn et al. (Mehlhorn et al. 1996). The F198W mutant was constructed by site directed mutagenesis of pIngPrP using a QuikChange® kit (Stratagene) according to the manufacturer's instructions. More specifically, the complimentary mutagenic primers (HaPrPF198W.F, 5′-CCACCAAGGGGGAGAACTGGACGGAGACCGACATC-3′ and HaPrPF198W.R, 5′-GATGTCGGTCTCCGTCCAGTTCTCCCCCTTGGTGG-3′) were synthesised and purified by HPLC (GIBCO BRL). The mutagenesis reaction was performed in a thermal cycler using the following conditions: 1 cycle of (30 s at 95°C) and 15 cycles of (30 s at 95°C, 1 min at 55°C and 11 min at 68°C). Mutant clones were identified by DNA sequencing. The wild-type protein and F198W variant were expressed in a protease-deficient strain of *Escherichia coli* (27C7) and purified as described previously (Kazlauskaite et al. 2003; Mehlhorn et al. 1996; Sanghera and Pinheiro 2002). During purification, wild-type and variant proteins were refolded under oxidizing conditions, producing the α-helical conformation of PrP as described previously (Kazlauskaite et al. 2003; Mehlhorn et al. 1996). The purity of the final product was determined by SDS-polyacrylamide gel electrophoresis and electrospray ionisation mass spectrometry, and was found to be over 95%. PrP concentration was determined spectrophotometrically, using $\varepsilon_{280} = 24{,}420\ M^{-1}cm^{-1}$ for the wild-type protein and $\varepsilon_{280} = 30{,}110\ M^{-1}cm^{-1}$ for the F198W variant (Gill and von Hippel 1989).

Fluorescence and denaturant unfolding

Fluorescence spectra were recorded on a Photon Technology International spectrofluorimeter using an excitation wavelength at 295 nm and a bandwidth of 2 nm (excitation

and emission slits). Typically, four scans were averaged per spectrum. Corresponding appropriate backgrounds of buffer alone or buffer and denaturant were subtracted from final spectra. In a typical unfolding experiment, two stock solutions of PrP at identical protein concentrations (4 μM) were prepared: one in buffer only (native protein) and one in buffer containing 6 M GdnHCl (unfolded protein). The buffers were 20 mM sodium acetate for pH 5.5 or 20 mM sodium phosphate for pH 7.0. For an unfolding curve the sample of unfolded protein was titrated (in increments of approximately 0.2 M GdnHCl) to a sample of native protein in a 1-cm pathlength cuvette. Fluorescence spectra were recorded immediately after the two solutions were mixed. A longer incubation was not necessary, as the system reaches equilibrium in less then 1 s, due to the very fast unfolding/refolding of the PrP (Apetri and Surewicz 2002; Wildegger et al. 1999). For each fluorescence emission spectrum obtained at an individual denaturant concentration, the wavelength of the peak was determined (λ_{max}). These values were normalised to fraction of folded protein (f_N) using the equation: $f_N = (y_D - y)/(y_D - y_N)$ (Pace 1986), where y_D is the λ_{max} of the fluorescence spectrum measured for protein in the denatured state, y is λ_{max} measured at a particular denaturant concentration, and y_N is the λ_{max} of protein in the native state. The f_N value was plotted as a function of GdnHCl concentration to give unfolding and refolding transition curves. Data were analysed according to a two-state model ($N \leftrightarrow U$, where N represents the native state of the protein and U the unfolded state). The free energy of folding in the absence of denaturant (ΔG°) was calculated by assuming that the free energy of folding ($\Delta G(D)$) is linearly dependent on denaturant concentration, according to the equation: $\Delta G(D) = \Delta G^\circ - m[D]$, where m is a constant reflecting the gradient of a plot of $\Delta G(D)$ as a function of denaturant concentration (Santoro and Bolen 1988). For each concentration of GdnHCl the equilibrium constant ($K(D)$) of the native and unfolded states was calculated by $K(D) = K^\circ \cdot \exp(-m[D]/RT)$ where R is the universal gas constant and T is the absolute temperature (293 K) and K° is the folding equilibrium constant under native conditions. The fraction folded term (f_N) shown on the plots therefore corresponds to the expression $K(D)/(K(D) + 1)$. Data were fit to two-state transition curves calculated by non-linear least-squares regression, using SigmaPlot (Systat Software, Richmond, CA, USA).

Circular dichroism

Far-UV CD spectra were collected on a JASCO J-715 spectropolarimeter using quartz cells of 1-mm pathlength. Typically, spectra were collected in continuous scanning mode at a scanning rate of 100 nm/min, a time constant of 1 s, a bandwidth of 2 nm and a resolution of 0.5 nm. Spectra were measured at 20°C on samples containing 5–7 μM protein. Typically, final spectra are an average of 16 scans and have the appropriate buffer background subtracted.

Pressure-jump measurements

Pressure-jump experiments were performed on a home-built apparatus described elsewhere (Pearson et al. 2002). A 50 μl sample is loaded into a chamber consisting of a sapphire ring that is closed off at both ends. A small pre-pressure (10–20 bar) is applied to remove elasticity from the system, before pressure is quickly applied and released (up to 400 bar in ~100 μs), using a piezo electric crystal stack (P-245.70 from Physik Instrumente GmbH, Waldbronn, Germany). Pressure application/release deforms the polyimide membrane that seals one end of the sample chamber. Fluorescence transients resulting from both pressure application (up to 400 bar) and release (to 10–20 bar) are recorded in each experiment. Excitation light from a 100-W Xe/Hg arc lamp (Hamamatsu Photonics, Enfeld, UK) is delivered via a light guide that abuts directly onto the sample chamber. Emission light is measured using a photomultiplier unit, abutting the sample cell at 90° to the light guide. The photomultiplier unit is based on an R928HA Hammamatsu photomultiplier with an added transimpedance pre-amp stage. Data collection is via an A/D board (DAS 50; Keithley Instruments Reading, UK), using specially developed software (J. Huber, Max-Planck-Institut, Dortmund). Multiple transients can be averaged using this system, which also uses over-sampling to make the most of the 1-MHz maximum acquisition rate. Transients can be repeated up to a maximum repetition rate of 12.5 times per second. Pressure is measured using a piezoelectric sensor (6158A from Kistler Instrumente AG, Winterthur, Switzerland).

Pressure-jump measurements were carried out at a protein concentration of 1 or 10 μM. Each measurement was the result of at least 1,000 repeats. Pressure step sizes of 350 bar were routinely used. Protein tryptophan fluorescence was recorded using an excitation light beam at 295 nm with a bandwidth of 1.8 nm and the emitted light was collected through a WG320 cut-off filter (Schott GmbH, Mainz, Germany), which excludes scattered excitation light below 320 nm.

Analysis of folding kinetics

Fluorescence transients resulting from pressure-jump experiments were fitted to a single exponential decay function of the form $F(t) = F_\infty + A_2[1 - \exp(-t/\tau_2)]$, where $F(t)$ is the fitted fluorescence function, F_∞ is the

end-point, A_2 is the amplitude and τ_2 is the time constant. The fluorescence data included a fast phase too fast to resolve, i.e. its time course coincided with the fast pressure step (see Sect. "Results"). Therefore the exponential function was used to fit the slower phase beginning at the end of the initial fast pressure step, about 100 μs after the start of the pressure step. The reciprocal time constants ($1/\tau_2$) resulting from pressure-jump measurements over a range of GdnHCl concentrations were fit to a two-state folding model according to: $1/\tau_2 = k_f \exp(m_f[D]/RT) + k_u \exp(m_u[D]/RT)$, where m_f and m_u are the kinetic folding and unfolding m-values, respectively, k_f and k_u are the folding and unfolding rate constants in the absence of denaturant, $[D]$ is the concentration of denaturant (in this case GdnHCl), R is the gas constant, and T is the absolute temperature (293 K). Fitting was carried out using data that was transformed to $\ln(1/\tau_2)$ to avoid undue bias towards large values. The minima of the chevron fits were determined by solving the differential, which resulted in the formula: $[D]_{min} = RT/(m_f - m_u) \ln(-m_u \cdot k_u/m_f \cdot k_f)$. The mid-point of the corresponding equilibrium ($[D]_{50\%}$) unfolding curve was calculated according to the following expression: $[D]_{50\%} = RT/(m_f - m_u) \ln(k_u/k_f)$.

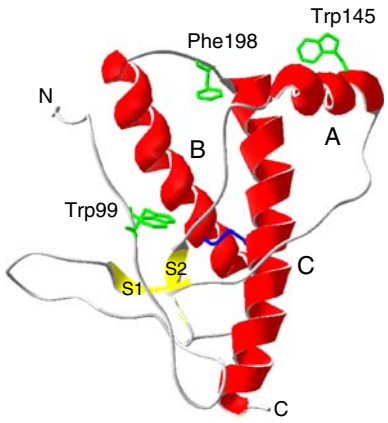

Fig. 1 Structure of the prion protein PrP(90–231). Ribbon representation of the folded C-terminal domain of SHaPrP(90–231) based on the NMR structure in aqueous solution (James et al. 1997). The N- and C-termini are labelled N and C, respectively; the three main helices A, B and C running from the N- to the C-terminus are shown in *red*, and the strands S1 and S2 of the short anti-parallel *β*-sheet are drawn in *yellow*. Using stick representation, the native tryptophan residues, Trp99 and Trp145, and phenylalanine Phe198 are highlighted in *green*, and the disulphide bond between Cys179 and Cys214 is shown in *blue*. The picture was generated using the PDB file 1B10 and the program Swiss-PDB Viewer (Guex and Peitsch 1997)

Results

F198W mutant has a native fold and an enhanced fluorescence

Tryptophan fluorescence spectroscopy is the most widely used spectroscopic tool to follow folding transitions of proteins, but it requires that the reporter Trp residues undergo a substantial change in their fluorescence properties upon the folding transition. In PrP(90-231) the two naturally occurring Trp residues in the hamster sequence, Trp 99 and 145, are exposed to solvent (Fig. 1). The fluorescence spectrum of folded PrP in aqueous solution shows an emission maximum (λ_{max}) around 344 nm at both pH 5.5 and 7.0 (Fig. 2). These λ_{max} values are characteristic of exposed tryptophans in native proteins (Lakowicz 1999). Unfolding of PrP with GdnHCl results in a red shift of the λ_{max} of about 6 nm and an increase in fluorescence intensity (Fig. 2). These small spectral changes make the intrinsic fluorescence of the wild-type protein a poor tool for refolding studies.

In order to enhance the fluorescence changes in folding experiments we have introduced a conservative mutation in PrP, where a phenylalanine residue (Phe198) was replaced with a tryptophan (F198W). Fluorescence spectra for the F198W variant protein are up to three times more intense than those for wild-type under native conditions (Fig. 2). In addition, folded F198W shows a λ_{max} at around 339 nm at both pH 7.0 and 5.5, consistent with the more buried position of Trp198 in the mutant protein, which results in a red shift for the λ_{max} of around 12 nm upon unfolding in GdnHCl.

Far-UV CD showed that the F198W variant folds to a similar state observed for the wild-type protein. CD spectra for the wild-type and variant proteins exhibit the typical bands for α-helix at 208 and 222 nm, both at pH 5.5 (Fig. 3) and pH 7.0 (data not shown).

Equilibrium unfolding and refolding of PrP

The effects of the F198W mutation on the equilibrium unfolding and refolding behaviour of the protein were investigated. Equilibrium unfolding and refolding experiments were carried out at varying concentrations of GdnHCl at pH 5.5 and 7.0 and monitored by Trp fluorescence. Unfolding and refolding of the F198W variant resulted in smooth reversible transition curves (Fig. 4). Two-state analysis of the unfolding/refolding transitions of F198W yielded the thermodynamic parameters shown in Table 1. The difference between the refolding equilibrium constants under native conditions ($K°$) and the midpoints of unfolding ($[D]_{50\%}$) at pH 5.5 and 7.0 reveals that PrP is more stable at the higher pH. Although the transition is best-described by a two-state model, the broadness of the concentration-range of denaturant as indicated by the m-values of 7.5 and 9.4 kJ mol^{-1} M^{-1}, for unfolding at pH

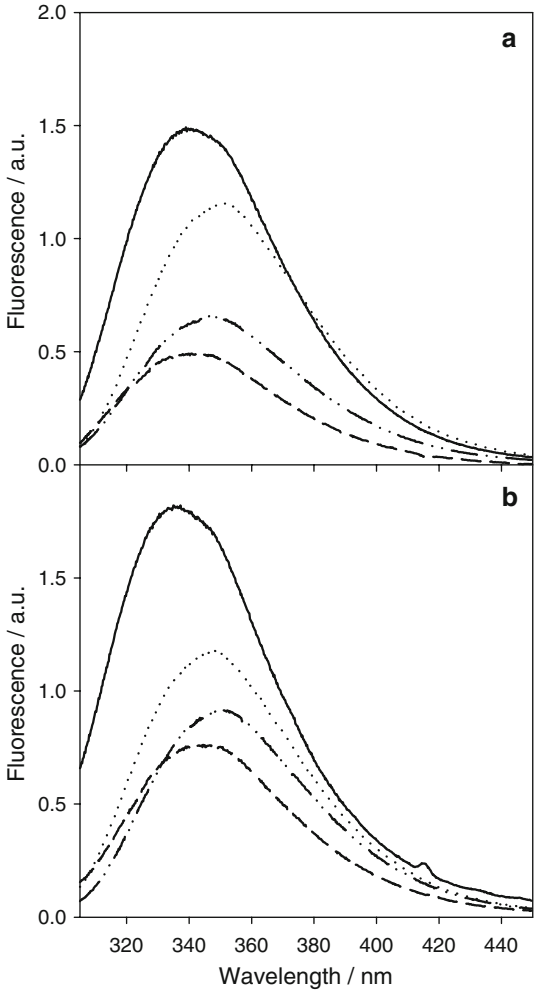

Fig. 2 Fluorescence enhancement of F198W mutant PrP. The fluorescence spectra at pH 5.5 (**a**) and pH 7.0 (**b**) for F198W mutant protein (*solid and dotted lines*) are compared with those for wild-type PrP (*dashed and dash-dotted lines*) in their native (*solid and dashed lines*) and denatured (*dotted and dash-dotted lines*) states. Protein concentration was 10 μM in 20 mM acetate (pH 5.5) or Tris (pH 7.0) buffers for the native state. Denatured states of PrP are in 4 M GdnHCl

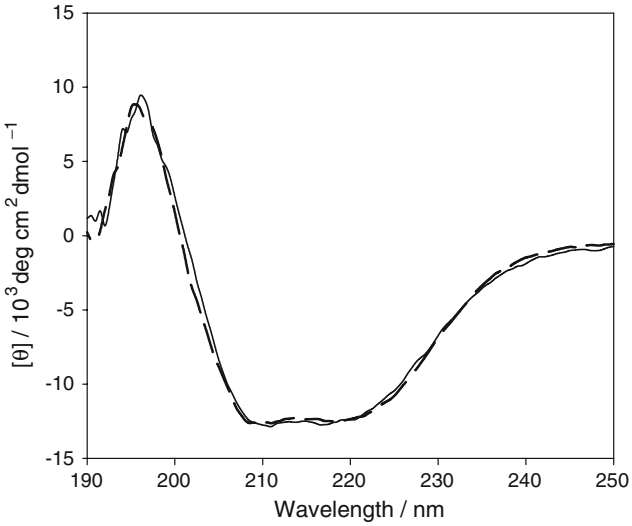

Fig. 3 F198W mutant PrP has a native fold. Far-UV CD spectra of F198W mutant (*solid line*) and wild-type PrP (*dashed line*) at pH 5.5. The concentration of PrP was 10 μM

5.5 and 7.0, respectively, indicates that the folding of PrP is not highly cooperative, and hence may not fold via a simple two-state mechanism.

Fast folding kinetics

The PrP exhibits broad unfolding and refolding transitions over the concentration range from 1 to 2.7 M GdnHCl (Fig. 4). We used this range of GdnHCl to examine the folding kinetics of F198W following a rapid pressure jump. Pressure application induced a decrease in fluorescence of 9% at pH 7 (Fig. 5a), indicating that the equilibrium folding transition was shifted towards the unfolded state (Fig. 2). Upon pressure release, the fluorescence signal recovered to its initial value, showing that folding is reversible.

The results of pressure-jump experiments on 10 μM F198W at a GdnHCl concentration of 1.7 M are shown in Fig. 5. The pressure profiles show that the change in pressure was 90% complete within 100 μs, and the final pressure remained constant during the measurements. Pressure application resulted in a two phase fluorescence response following a spike in the fluorescence signal that preceded the rise in pressure. This spike is the result of an electrical artefact that has been documented before (Pearson et al. 2002). After pressure application, a very fast phase of fluorescence quenching was observed, too fast to be resolved ($1/\tau_1 > 20{,}000\ s^{-1}$), followed by a second phase of further quenching of fluorescence that was well described by a single exponential function ($A_2 = 7.3\%$, $1/\tau_2 = 1{,}480\ s^{-1}$). Upon pressure release, the transient was essentially reversed with little difference in kinetic parameters.

The dependence of the folding kinetic parameters (reciprocal time constants and amplitudes) was first investigated at various pressure step sizes (Fig. 6), in order to establish the limits to the linear response range of our measurements with PrP. The amplitude of the fast phase showed a linear correlation with the pressure step-size over the entire range tested, and the amplitude of the exponential phase showed also a linear response up to pressure step sizes of 350 bar (Fig. 6b). The inverse time constants of the exponential phase showed no significant dependence on pressure step-size for pressure release measurements, but increased with step-size on pressure application measurements (Fig. 6a), indicating the presence of a significant activation volume

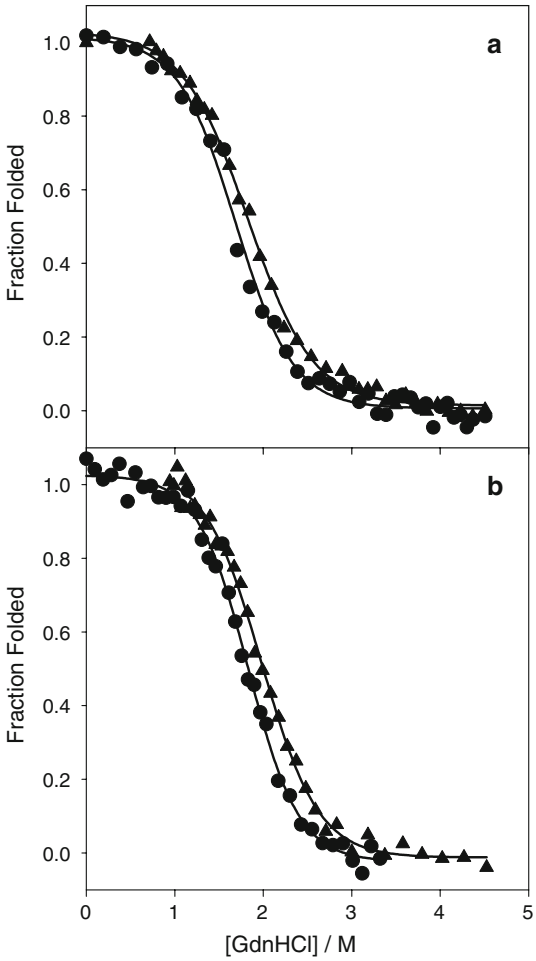

Fig. 4 Denaturant unfolding and refolding of PrP. Typical unfolding (*circles*) and refolding (*triangles*) equilibrium curves for F198W PrP as a function of GdnHCl concentrations at pH 5.5 (**a**) and 7.0 (**b**). Curves were determined from blue shift of λ_{max} for fluorescence spectra at the various denaturant concentrations (see Sect. "Materials and methods"). The protein concentration was 4 μM in sodium acetate or phosphate buffers

for at least one of the component folding or unfolding steps. We can estimate the size of this apparent activation volume from this pressure dependence using the equation: $\Delta V^{\ddagger}_{app} = -RT \cdot \partial \ln k / \partial P$, to be −4.9 ml mol^{-1}. This value represents an absolute minimum, since there may be multiple reaction steps with partially compensatory activation volumes.

Pressure-jump experiments (350 bar) were performed over a range of GdnHCl concentrations (0.9–3.2 M) at pH 7.0. Outside this range of GdnHCl concentrations the amplitude of the exponential phase was too small to measure (<1%). Typical transients resulting from pressure application are shown in Fig. 7. The same two-phase quench in fluorescence was observed over the entire range of GdnHCl concentrations studied here. The pressure release results were the reverse of the results of pressure application (data not shown). The amplitude of the fast phase varied little over the range of GdnHCl concentrations tested.

Graphs of reciprocal time constants against GdnHCl concentration produced chevron plots (Fig. 8a). A systematic difference between the results from pressure application and pressure release was observed. At low GdnHCl concentrations reciprocal relaxation times resulting from pressure release were faster than pressure application but the reverse was observed at high GdnHCl concentrations. Therefore the data was fitted separately for pressure application and pressure release, using a two-state folding model. The results of these analyses are summarised in Table 2. Chevron plots from pressure application are shifted to lower GdnHCl concentrations by 0.35 M at pH 7.0 (0.25 M at pH 5.5), compared with the chevron for pressure release. This result is consistent with pressure application shifting the equilibrium towards the unfolded state.

The plots of amplitudes of the exponential phase against the denaturant concentration are shown in Fig. 8b. Typical amplitude plots of single step reactions show highest values where the equilibrium constant is closest to 1, i.e. close to the minimum of the chevron plot (given that the values for m_u and m_f are not very far apart) (Fig. 8). However, an interesting profile of amplitudes is observed with double maxima (Fig. 8b). The first maximum at ∼1.7 M GdnHCl is close to the chevron minima for pressure application data (Fig. 8a and Table 2) and the equilibrium $[D]_{50\%}$ values (Table 1). A second maximum at 2.3 M GdnHCl at pH 7.0 or 2.1 M GdnHCl at pH 5.5 is close to the corresponding

Table 1 Equilibrium parameters for denaturant unfolding and refolding of the prion protein, PrP(90–231)

	pH 5.5		pH 7.0	
	Unfolding	Refolding	Unfolding	Refolding
$K°$	196 ± 50	174 ± 25	1193 ± 358	1084 ± 232
m (kJ mol^{-1} M^{-1})	7.5 ± 0.3	6.7 ± 0.2	9.4 ± 0.4	8.5 ± 0.3
$[D]_{50\%}$ (M)	1.9 ± 0.2	1.7 ± 0.1	1.8 ± 0.2	2.0 ± 0.1

Equilibrium parameters were calculated through a two-state folding analysis of the equilibrium unfolding and refolding plots (see Sect. "Materials and methods")

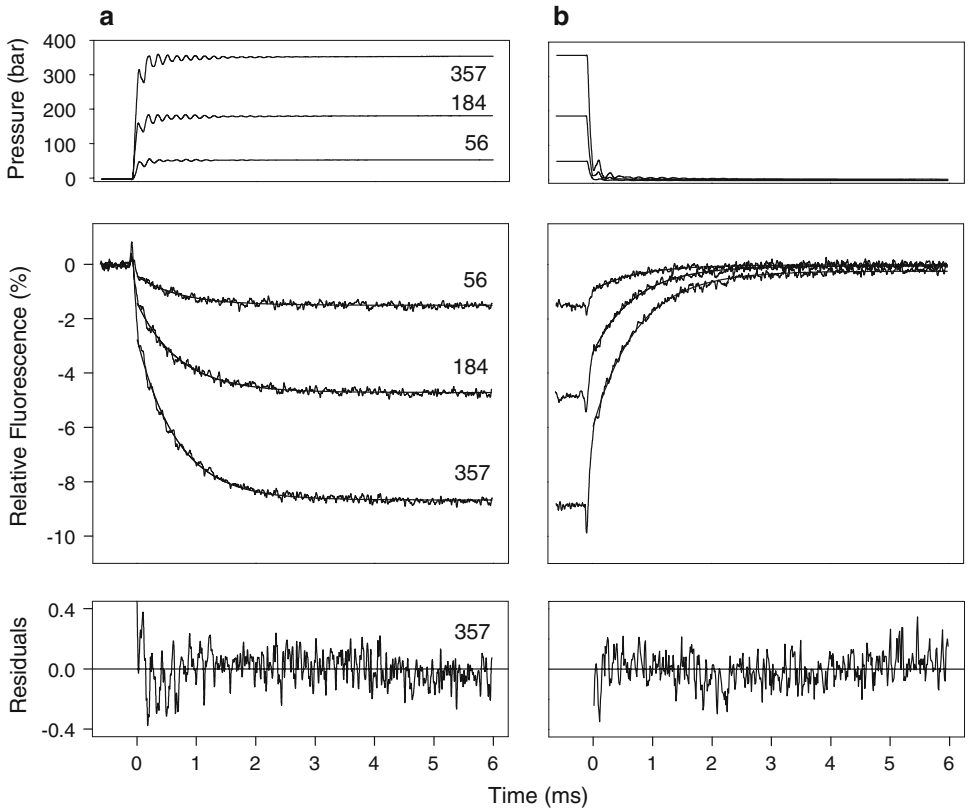

Fig. 5 Folding kinetics after pressure-jump. **a** Unfolding and **b** refolding of 10 μM F198W protein for 1.7 M GdnHCl at 20°C, pH 7.0 following pressure application (**a**) and release (**b**). *Numbers* next to transients indicate the size of the pressure step in bar. *Top panels* show the profiles of the pressure jumps. Single exponential fits to example transients are shown in the *middle panels*. *Bottom panels* show typical residuals of the fitting analysis

chevron minimum for the pressure release measurements (Table 2).

The results from pressure application and release mirror each other quite closely, though the amplitudes due to pressure application are consistently larger than the amplitudes due to pressure release. Overall, the transients were completely reversible in total amplitude, implying that there is a shift in the equilibrium position between populations that are responsible for the fast phase and the exponential phase.

Discussion

A key molecular event in the pathogenesis of prion diseases is the conversion of PrP^{C} to disease-associated form of the protein PrP^{Sc} (Bolton et al. 1982; Prusiner 1998). While this event has yet to be characterised, it is possible that PrP^{Sc} is formed by recruitment of a partially-folded intermediate on the folding pathway of PrP^{C} (Cohen et al. 1994). The presence of equilibrium folding intermediates for the folding of PrP has been a controversial issue (Hornemann and Glockshuber 1998; Swietnicki et al. 1997, 2000), but NMR (Hosszu et al. 2005; Kuwata et al. 2002; Nicholson et al. 2002) and fluorescence experiments (Cordeiro et al. 2005b; Jenkins et al. 2008) are now providing evidence that an intermediate may indeed be present. Kinetic studies also support this view (Apetri et al. 2004, 2006; Apetri and Surewicz 2002).

To further investigate the folding mechanism of PrP we made a mutant of the truncated form of the Syrian hamster PrP with an extra tryptophan residue to improve the fluorescence properties of the protein. Far-UV CD showed that this mutation is not detrimental to the folding of PrP. Analysis of unfolding transition curves revealed a small destabilisation at pH 5.5 relative to pH 7.0, consistent with previous reports (Hornemann and Glockshuber 1998; Swietnicki et al. 1997). This observation is also in line with previous suggestions that the conversion of PrP^{C} to PrP^{Sc} may occur under the acidic conditions found in the endosomal pathway (Borchelt et al. 1992; Caughey et al. 1991), through partial destabilisation of the protein fold.

Where past investigations of the kinetics of the folding of PrP have relied on slowing the reaction by conducting experiments at low temperatures (Apetri et al. 2004, 2006; Apetri and Surewicz 2002; Wildegger et al. 1999), here we have employed novel pressure-jump technology and carried out kinetic measurements at 20°C. In agreement with previous kinetic studies (Apetri et al. 2004; Apetri and Surewicz 2002; Wildegger et al. 1999), the recorded transients display a fast exponential phase, preceded by an even faster phase too rapid to model. The presence of a fast phase is indicative of the formation of a folding intermediate early in the folding process (Roder and Colon 1997).

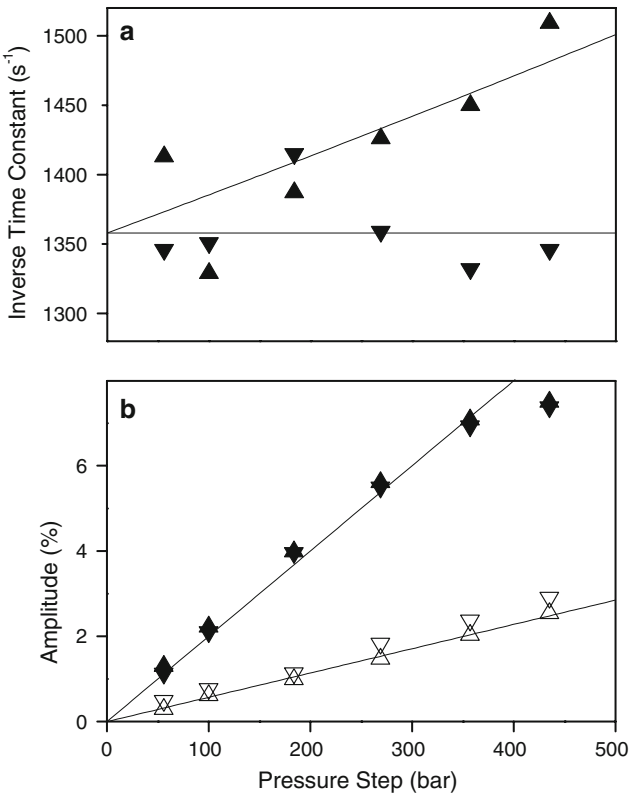

Fig. 6 Effect of the size of the pressure step. **a** Reciprocal time constants and **b** amplitudes observed upon pressure application (*upward triangles*) and release (*downward triangles*). *Filled symbols* represent results from the exponential phase, whilst the *empty symbols* in (**b**) are the amplitudes of the fast phase

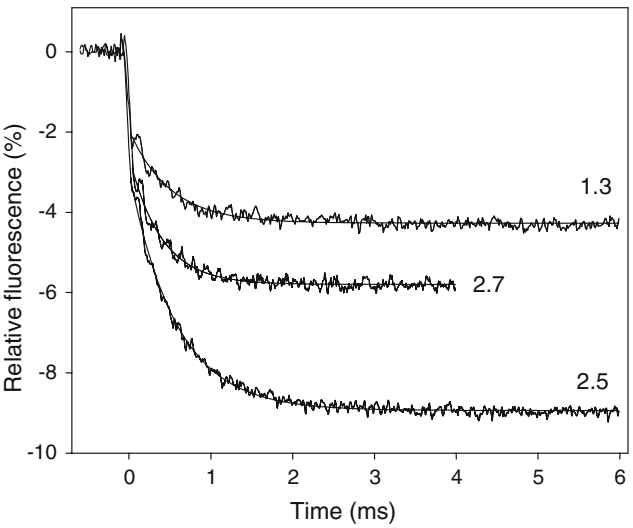

Fig. 7 Example transients from fast pressure application. Transients shown were obtained using 10 μM F198W in 20 mM MOPS, pH 7.0 at 20°C. *Numbers* next to transients indicate the [GdnHCl] in molar units. Single exponential fits to the fluorescence decays overlay the data

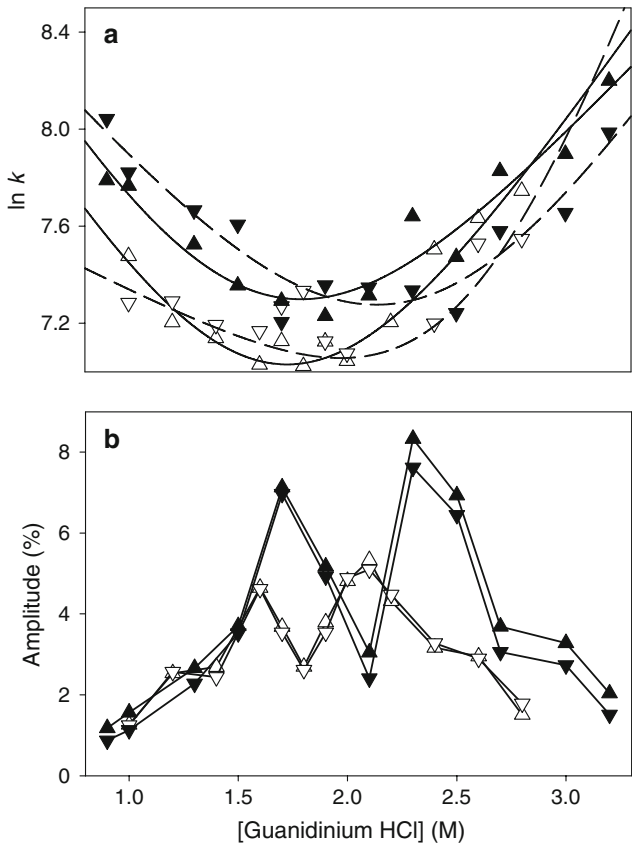

Fig. 8 GdnHCl-dependence of folding kinetics of F198W prion mutant. **a** Reciprocal time constants and **b** amplitudes as a function of GdnHCl concentration derived from pressure-jump relaxation experiments. *Filled symbols* are results of experiments at pH 7.0 whereas *open symbols* are results from pH 5.5 for pressure application (*upward triangles*) and pressure release (*downward triangles*). Amplitudes in *panel* **b** are expressed as percentage change in fluorescence. The chevrons in *panel* **a** illustrate the analysis of the experimental data points according to a linear two-state folding model (see Sect. "Materials and methods")

A continuous-flow study of the fast folding kinetics of PrP at 5°C showed two kinetic phases (Apetri et al. 2006). In contrast, our pressure-jump transients collected at 20°C are described by a single-exponential phase. The measurements at low temperature produced roll-over of chevron plots and two-phase kinetics indicative of the formation of a folding intermediate. Flow techniques are able to function at denaturant concentrations far removed from the poised equilibrium position necessary for perturbation experiments, such as pressure jump, and are therefore more suited to observation of chevron roll-overs. Pressure jump, on the other hand, allows data to be gathered at room temperature and additionally permits information on activation volumes to be determined.

Previous equilibrium folding studies of PrP have used pressure as a denaturant to study the 'folding landscape' of the protein, revealing alternative conformations which

Table 2 Kinetic parameters for the folding of the prion protein, PrP(90–231)

	pH 5.5		pH 7.0	
	Pressure application	Pressure release	Pressure application	Pressure release
k_f (s^{-1})	6003	2441	8103	6634
m_f (kJ mol^{-1} M^{-1})	-3.4 ± 1.4	-1.1 ± 0.7	-3.6 ± 1.2	-2.4 ± 0.7
k_u (s^{-1})	67	1.34	164	36.6
m_u (kJ mol^{-1} M^{-1})	3.1 ± 0.87	6.0 ± 3.2	2.3 ± 0.6	3.2 ± 1.1
$[D]_{min}$ (M)	1.73	1.97	1.79	2.13
$[D]_{50\%}$ (M)	1.69	2.57	1.61	2.26

Kinetic parameters were calculated through a two-state folding analysis of chevron plots (see Sect. "Materials and methods"), where k_f and k_u are the folding and unfolding rate constants, respectively, in the absence of denaturant; m_f and m_u are the kinetic folding and unfolding *m*-values, respectively; and $[D]$ is the concentration of denaturant, GdnHCl

could be recruited to a pathogenic species (Alvarez-Martinez et al. 2003; Cordeiro et al. 2005b,c; Font et al. 2006; Kuwata et al. 2002). Here, pressure-jump technology has, for the first time, been applied to study the kinetics of the folding of PrP. This has been made possible by the use of pressure-jumps of 350 bar which reach completion within 100 μs, in contrast to apparatus that delivers a larger pressure step size but within a time-frame of over 5 ms (DeArmond et al. 1997). However, the equilibrium studies conducted previously found that pressures of around 4,000 bar must be applied to fully unfold PrP. For this reason these kinetic experiments used the denaturant GdnHCl at concentrations ranging across the equilibrium folding curves to poise the equilibrium close to unity so that an appreciable relative change in the equilibrium position might be observed with the application and release of pressure. This method has been employed successfully in folding studies of staphylococcal nuclease (Vidugiris et al. 1996) and a fast-folding cold-shock protein (Jacob et al. 1999). The pressure-jump technique enables the study of volume changes over the course of a folding reaction. Equilibrium pressure studies have determined the volume change with unfolding of α-helical SHaPrP(90–231) to be -31.9 ml mol^{-1} (Font et al. 2006). However, the relatively small range of pressure step-sizes accessible in this study prevented the determination of the activation volume, a parameter analogous to the activation energy of a reaction, providing further insight on the folding pathway of PrP.

The presence of a double maximum in the plots of amplitudes of the exponential phase against the denaturant concentration is intriguing. It contrasts with the classic bell-shaped curve expected for a single-step transition. It is worth emphasising that this feature was observed at two different pH values, indicating that the observation of the double maximum is not an experimental artefact. Attempts to fit these results to models of unfolding that included unfolding intermediates met with partial success. Whilst it is possible to reproduce this 'twin peaks' feature using this method, there was no set of global parameters that could fit both the amplitude and reciprocal rate constant plots simultaneously. Additionally, models including significant amounts of on-pathway folding intermediates yielded non-sigmoidal unfolding curves, which did not represent the observed experimental transitions. We conclude from this that multiple folding intermediates are necessary to explain these data. However, the presence of three tryptophan residues may also be a contributor to the complex behaviour of the observed amplitudes. In future, the use of single tryptophan variants of PrP is likely to provide further insights on the system. We have presented the first use of pressure-jump to study the folding kinetics of PrP. The results are in broad agreement with results from flow-based techniques and provide further insight into the folding mechanism of PrP. The techniques introduced could be used to asses the effects of disease-associated mutants of PrP or potential structure stabilizing ligands to prevent prion conversion.

Acknowledgments We thank Andrew Gill (IAH, Compton) for mass spectrometry of mutant prion proteins, and Matthew Hicks for advice on protein folding experiments. This work has been supported by the Wellcome Trust (SHoWCAse 053914/Z/98/Z to TJTP and programme grant 07021 to MAG), the Biotechnology and Biological Sciences Research Council (88/BS516471), the Engineering and Physical Sciences Research Council (DCJ studentship) and the Royal Society.

References

Alvarez-Martinez MT, Torrent J, Lange R, Verdier JM, Balny C, Liautard JP (2003) Optimized overproduction, purification, characterization and high-pressure sensitivity of the prion protein in the native (PrP^C-like) or amyloid (PrP^{Sc}-like) conformation. Biochim Biophys Acta 1645:228–240

Apetri AC, Surewicz WK (2002) Kinetic intermediate in the folding of human prion protein. J Biol Chem 277:44589–44592. doi: 10.1074/jbc.C200507200

Apetri AC, Surewicz K, Surewicz WK (2004) The effect of disease-associated mutations on the folding pathway of human prion

protein. J Biol Chem 279:18008–18014. doi:10.1074/jbc.M313581200

Apetri AC, Maki K, Roder H, Surewicz WK (2006) Early intermediate in human prion protein folding as evidenced by ultrarapid mixing experiments. J Am Chem Soc 128:11673–11678. doi:10.1021/ja063880b

Bolton DC, McKinley MP, Prusiner SB (1982) Identification of a protein that purifies with the scrapie prion. Science 218:1309–1311. doi:10.1126/science.6815801

Borchelt D, Taraboulos A, Prusiner S (1992) Evidence for synthesis of scrapie prion proteins in the endocytic pathway. J Biol Chem 267:16188–16199

Caughey B, Raymond GJ, Ernst D, Race RE (1991) N-terminal truncation of the scrapie-associated form of PrP by lysosomal protease(s): implications regarding the site of conversion of PrP to the protease-resistant state. J Virol 65:6597–6603

Chesebro B, Race R, Wehrly K, Nishio J, Bloom M, Lechner D, Bergstrom S, Robbins K, Mayer L, Keith JM, Garon C, Haase A (1985) Identification of scrapie prion protein-specific mRNA in scrapie-infected and uninfected brain. Nature 315:331–333. doi:10.1038/315331a0

Cohen FE, Pan KM, Huang Z, Baldwin M, Fletterick RJ, Prusiner SB (1994) Structural clues to prion replication. Science 264:530–531. doi:10.1126/science.7909169

Collinge J (2005) Molecular neurology of prion disease. J Neurol Neurosurg Psychiatry 76:906–919. doi:10.1136/jnnp.2004.048660

Cordeiro Y, Kraineva J, Gomes M, Lopes M, Martins VR, Lima L, Foguel D, Winter R, Silva JL (2005a) The amino-terminal PrP domain is crucial to modulate prion misfolding and aggregation. Biophys J 89:2667–2676. doi:10.1529/biophysj.105.067603

Cordeiro Y, Kraineva J, Gomes MP, Lopes MH, Martins VR, Lima LM, Foguel D, Winter R, Silva JL (2005b) The amino-terminal PrP domain is crucial to modulate prion misfolding and aggregation. Biophys J 89:2667–2676. doi:10.1529/biophysj.105.067603

Cordeiro Y, Kraineva J, Winter R, Silva JL (2005c) Volume and energy folding landscape of prion protein revealed by pressure. Braz J Med Biol Res 38:1195–1201. doi:10.1590/S0100-879X2005000800006

DeArmond SJ, Sanchez H, Yehiely F, Qiu Y, Ninchak-Casey A, Daggett V, Camerino AP, Cayetano J, Rogers M, Groth D, Torchia M, Tremblay P, Scott MR, Cohen FE, Prusiner SB (1997) Selective neuronal targeting in prion disease. Neuron 19:1337–1348. doi:10.1016/S0896-6273(00)80424-9

Donne DG, Viles JH, Groth D, Mehlhorn I, James TL, Cohen FE, Prusiner SB, Wright PE, Dyson HJ (1997) Structure of the recombinant full-length hamster prion protein PrP(29-231): the N terminus is highly flexible. Proc Natl Acad Sci USA 94:13452–13457. doi:10.1073/pnas.94.25.13452

Font J, Torrent J, Ribo M, Laurents DV, Balny C, Vilanova M, Lange R (2006) Pressure-jump induced kinetics reveals a hydration dependent folding/unfolding mechanism of ribonuclease A. Biophys J 91:2264–2274

Gill SC, von Hippel PH (1989) Calculation of protein extinction coefficients from amino acid sequence data. Anal Biochem 182:319–326. doi:10.1016/0003-2697(89)90602-7

Guex N, Peitsch MC (1997) SWISS-MODEL and the Swiss-PdbViewer: an environment for comparative protein modeling. Electrophoresis 18:2714–2723. doi:10.1002/elps.1150181505

Hornemann S, Glockshuber R (1998) A scrapie-like unfolding intermediate of the prion protein domain PrP(121-231) induced by acidic pH. Proc Natl Acad Sci USA 95:6010–6014. doi:10.1073/pnas.95.11.6010

Hosszu LL, Wells MA, Jackson GS, Jones S, Batchelor M, Clarke AR, Craven CJ, Waltho JP, Collinge J (2005) Definable equilibrium states in the folding of human prion protein. Biochemistry 44:16649–16657. doi:10.1021/bi051277k

Jackson GS, Hill AF, Joseph C, Hosszu LL, Power A, Waltho JP, Clarke AR, Collinge J (1999) Multiple folding pathways for heterologously expressed human prion protein. Biochim Biophys Acta 1431:1–13

Jacob M, Holtermann G, Perl D, Reinstein J, Schindler T, Geeves MA, Schmid FX (1999) Microsecond folding of the cold shock protein measured by a pressure-jump technique. Biochemistry 38:2882–2891. doi:10.1021/bi982487i

James TL, Liu H, Ulyanov NB, Farr-Jones S, Zhang H, Donne DG, Kaneko K, Groth D, Mehlhorn I, Prusiner SB, Cohen FE (1997) Solution structure of a 142-residue recombinant prion protein corresponding to the infectious fragment of the scrapie isoform. Proc Natl Acad Sci USA 94:10086–10091. doi:10.1073/pnas.94.19.10086

Jenkins DC, Sylvester ID, Pinheiro TJ (2008) The elusive intermediate on the folding pathway of the prion protein. FEBS J 275:1323–1335. doi:10.1111/j.1742-4658.2008.06293.x

Kazlauskaite J, Sanghera N, Sylvester I, Venien-Bryan C, Pinheiro TJ (2003) Structural changes of the prion protein in lipid membranes leading to aggregation and fibrillization. Biochemistry 42:3295–3304. doi:10.1021/bi026872q

Kuwata K, Li H, Yamada H, Legname G, Prusiner SB, Akasaka K, James TL (2002) Locally disordered conformer of the hamster prion protein: a crucial intermediate to PrPSc? Biochemistry 41:12277–12283. doi:10.1021/bi026129y

Lakowicz JR (1999) Protein fluorescence, 2nd edn. Kluwer Academic/Plenum Publishers, New York

Liemann S, Glockshuber R (1999) Influence of amino acid substitutions related to inherited human prion diseases on the thermodynamic stability of the cellular prion protein. Biochemistry 38:3258–3267. doi:10.1021/bi982714g

Liu H, Farr-Jones S, Ulyanov NB, Llinas M, Marqusee S, Groth D, Cohen FE, Prusiner SB, James TL (1999) Solution structure of Syrian hamster prion protein rPrP(90-231). Biochemistry 38:5362–5377. doi:10.1021/bi982878x

McKinley MP, Bolton DC, Prusiner SB (1983) A protease-resistant protein is a structural component of the scrapie prion. Cell 35:57–62. doi:10.1016/0092-8674(83)90207-6

Mehlhorn I, Groth D, Stockel J, Moffat B, Reilly D, Yansura D, Willett WS, Baldwin M, Fletterick R, Cohen FE, Vandlen R, Henner D, Prusiner SB (1996) High-level expression and characterization of a purified 142-residue polypeptide of the prion protein. Biochemistry 35:5528–5537. doi:10.1021/bi952965e

Meyer RK, McKinley MP, Bowman KA, Braunfeld MB, Barry RA, Prusiner SB (1986) Separation and properties of cellular and scrapie prion proteins. Proc Natl Acad Sci USA 83:2310–2314. doi:10.1073/pnas.83.8.2310

Nicholson EM, Mo H, Prusiner SB, Cohen FE, Marqusee S (2002) Differences between the prion protein and its homolog doppel: a partially structured state with implications for scrapie formation. J Mol Biol 316:807–815. doi:10.1006/jmbi.2001.5347

Oesch B, Westaway D, Walchli M, McKinley MP, Kent SB, Aebersold R, Barry RA, Tempst P, Teplow DB, Hood LE et al (1985) A cellular gene encodes scrapie PrP 27-30 protein. Cell 40:735–746. doi:10.1016/0092-8674(85)90333-2

Pace CN (1986) Determination and analysis of urea and guanidine hydrochloride denaturation curves. Methods Enzymol 131:266–280. doi:10.1016/0076-6879(86)31045-0

Pan KM, Baldwin M, Nguyen J, Gasset M, Serban A, Groth D, Mehlhorn I, Huang Z, Fletterick RJ, Cohen FE, Prusiner SB (1993) Conversion of alpha-helices into beta-sheets features in the formation of the scrapie prion proteins. Proc Natl Acad Sci USA 90:10962–10966. doi:10.1073/pnas.90.23.10962

Pearson DS, Holtermann G, Ellison P, Cremo C, Geeves MA (2002) A novel pressure-jump apparatus for the microvolume analysis of protein–ligand and protein–protein interactions: its application to nucleotide binding to skeletal-muscle and smooth-muscle myosin subfragment-1. Biochem J 366:643–651. doi:10.1042/BJ20020462

Prusiner SB (1998) Prions. Proc Natl Acad Sci USA 95:13363–13383. doi:10.1073/pnas.95.23.13363

Prusiner SB, Scott MR, DeArmond SJ, Cohen FE (1998) Prion protein biology. Cell 93:337–348. doi:10.1016/S0092-8674(00)81163-0

Riek R, Hornemann S, Wider G, Billeter M, Glockshuber R, Wuthrich K (1996) NMR structure of the mouse prion protein domain PrP(121-321). Nature 382:180–182. doi:10.1038/382180a0

Roder H, Colon W (1997) Kinetic role of early intermediates in protein folding. Curr Opin Struct Biol 7:15–28. doi:10.1016/S0959-440X(97)80004-8

Sanghera N, Pinheiro TJ (2002) Binding of prion protein to lipid membranes and implications for prion conversion. J Mol Biol 315:1241–1256. doi:10.1006/jmbi.2001.5322

Santoro MM, Bolen DW (1988) Unfolding free energy changes determined by the linear extrapolation method. 1. Unfolding of phenylmethanesulfonyl alpha-chymotrypsin using different denaturants. Biochemistry 27:8063–8068. doi:10.1021/bi00421a014

Stahl N, Baldwin MA, Teplow DB, Hood L, Gibson BW, Burlingame AL, Prusiner SB (1993) Structural studies of the scrapie prion protein using mass spectrometry and amino acid sequencing. Biochemistry 32:1991–2002. doi:10.1021/bi00059a016

Swietnicki W, Petersen R, Gambetti P, Surewicz WK (1997) pH-dependent stability and conformation of the recombinant human prion protein PrP(90-231). J Biol Chem 272:27517–27520. doi:10.1074/jbc.272.44.27517

Swietnicki W, Petersen RB, Gambetti P, Surewicz WK (1998) Familial mutations and the thermodynamic stability of the recombinant human prion protein. J Biol Chem 273:31048–31052. doi:10.1074/jbc.273.47.31048

Swietnicki W, Morillas M, Chen SG, Gambetti P, Surewicz WK (2000) Aggregation and fibrillization of the recombinant human prion protein huPrP90-231. Biochemistry 39:424–431. doi:10.1021/bi991967m

Vidugiris GJA, Truckses DM, Markley JL, Royer CA (1996) High-pressure denaturation of staphylococcal nuclease proline-to-glycine substitution mutants. Biochemistry 35:3857–3864. doi:10.1021/bi952012g

Wildegger G, Liemann S, Glockshuber R (1999) Extremely rapid folding of the C-terminal domain of the prion protein without kinetic intermediates. Nat Struct Biol 6:550–553. doi:10.1038/9323

Zhang H, Stockel J, Mehlhorn I, Groth D, Baldwin MA, Prusiner SB, James TL, Cohen FE (1997) Physical studies of conformational plasticity in a recombinant prion protein. Biochemistry 36:3543–3553. doi:10.1021/bi961965r